SINGLE CRYSTAL SURFACE WORK FUNCTION AND DESORPTION STUDIES

Final Report

NGR 38-010-001

Submitted by

National Aeronautics and Space Administration

Washington, D. C. 20546

Submitted by

L. W. Swanson

and

R. W. Strayer

Linfield Research Institute
Linfield College
McMinnville, Oregon 97128

October 31, 1970

SINGLE CRYSTAL SURFACE WORK FUNCTION AND DESORPTION STUDIES

Final Report

NGR 38-010-001

Submitted to

National Aeronautics and Space Administration

Washington, D.C. 20546

Submitted by

L. W. Swanson

and

R. W. Strayer

Linfield Research Institute
Linfield College
McMinnville, Oregon 97128

October 31, 1970

RESEARCH OBJECTIVES

The research program reported here has two objectives: (1) measurement of single crystal face work function values for various metals of interest as collector surfaces in thermionic diodes, (2) measurement of adsorption and desorption characteristics of cesium on single crystal surfaces of selected refractory metals.

ABSTRACT

Using the field emission retarding potential method true work functions have been measured for the following substrates: Cu(100), $\phi_c = 5.10$; W(111), $\phi_c = 4.47$; Ir(111), $\phi_c = 5.76$ eV. The electron reflection coefficients from these surfaces have also been examined near zero volts. Preliminary measurements of sticking coefficients and desorption characteristics have been measured for cesium on 110 W. The results indicate a sticking coefficient of unity at a substrate temperature of 77°K for monolayer coverages. Evidence of discrete adsorption states along with continuous variation of binding energy with coverage is indicated by our thermal desorption results.

I

Work Function Measurements by the Field Emission Retarding Potential Method

INTRODUCTION

Of fundamental importance to the experimental and theoretical understanding of surfaces is the reliable measurement of its work function. Motivated by the advancing technology of electron emitting devices and more recently by progress in experimental and theoretical understanding of surfaces, an increasing number of measurements of clean, mono-crystal face work function have been reported. Primarily due to the perennial problem of surface purity and partly due to inadequacies in the theoretical description of the various modes of electron emission one finds an inordinate degree of disagreement in the literature values of work function. However, the rapid advance in the methodology of fabricating ultra pure metals along with the increasing number of ways of cleaning and sensitively detecting.

minute concentrations of surface impurities is gradually eliminating the surface contamination as a major factor in arriving at a consensus as to the appropriate clean mono-crystal face work function values. A further problem of lesser importance is that of maintaining a desired crystallographic orientation at the surface during the cleaning procedure; this problem can be detected by LEED analysis and occurs for relatively few materials.

It is in regards to the problem of the inadequacies of the existing models for various types of electron emission (e.g., thermionic, photo or field emission) to provide unambiguous values of mono-crystal face work function that has prompted this work. Here we are concerned not with contact potential difference measurement but rather with absolute (or true) work functions.

The primary electron emission processes whereby work function values of the emitter can be theoretically obtained are thermionic, photo electric and field emission. The assumptions, limitations and applicability of each of these methods for obtaining work function values have been adequately described in the literature. Suffice it to say that the Sommerfeld free electron model, which is the basic model utilized by the experimentalist for most electron emission processes, is severely strained in its application to a wide variety of non-free electron refractory metal emitters. This limitation is succinctly described for thermionic, field and photo electric emission

by Itskovich.[1] Recent field emission energy distribution measurements have given dramatic experimental evidence as to the inability of the Sommerfeld based Fowler-Nordheim theory to explain the results from all crystallographic directions of tungsten, molybdenum and copper emitters.[2,3,4] Besides the fundamental problem of model applicability, a host of minor complex effects such as the temperature dependence of the work function, variable reflection coefficients and the Schottky effect must be carefully incorporated into the theoretical framework of the emission process.

A method of measuring the true work function of an electron collector surface which circumvents most, if not all, of the above mentioned difficulties is the field electron retarding potential (FERP) method. The FERP approach, introduced many years ago by Henderson,[5] has been largely neglected* with the exception of a recent study of polycrystal surfaces by Holscher.[6] Yet this method and an experimentally complex adaptation of the Shelton method[7] are the only ways by which non-relative work functions of an electron collector surface can be measured. As will be shown in the following section, the success of the FERP method rests on the theoretical and experimen-

* It should be recognized that all of the many energy distribution studies utilizing retarding potential analyzers necessarily measure the collector work function as a matter of course, but only Henderson's and Holscher's work intentionally used the method as a work function measuring device.

tally verifiable fact that the voltage threshold for collection of field emitted electrons occurs at the Fermi level E_f at 0^oK or can be described by a Boltzman tail, i.e. $\exp (E_f - E)/kT$, at temperature T. The several experimental studies of the total energy distribution (TED) now in the literature[2, 8, 9] provide a firm basis for the validity of the preceeding fact; also if the appropriate crystallographic direction of a refractory metal emitter is employed, the free electron based Fowler-Nordheim model of field emission is adequate for this application.

In the following sections we shall describe the theoretical basis of the FERP method, its experimental application to the measurement of mono-crystal face work functions, and the results obtained from several substrates. An interesting and useful fallout from the experimental approach described here is the ability to detect structure in the reflection coefficient for impinging electrons from near zero to several volts energy.

THEORETICAL CONSIDERATIONS

The expression for the differential field emitted current dI_c between energy ε and $\varepsilon + d\varepsilon$ (where $\varepsilon = E - E_f$) in the case of a free electron model is given as follows:

$$dI_c/d\varepsilon = I_o e^{\varepsilon/d} / [(1 + e^{\varepsilon/pd}) d] \qquad (1)$$

where $p = kT/d$ is a dimensionless parameter. The value d is given by

$$d = \hbar eF/2(2m\phi_e)^{\frac{1}{2}} t(y) = 0.976F/\phi_e^{\frac{1}{2}}\, t(y) \quad (eV) \qquad (2)$$

where the electric field F and the emitter work function ϕ_e are in $V/\mathring{A}$ and eV, respectively. The maximum emitter current I_o in Eq. (1) is given by the well known Fowler-Nordheim equation

$$\begin{aligned} I_o &= \frac{e^3 F^2 A}{8\pi h \phi t^2(y)} \exp\left[-4(2m\phi^3)^{\frac{1}{2}} v(y)/3\hbar eF\right] \\ &= \frac{1.54 \times 10^{10}}{\phi t^2(y)} F^2 A \exp\left[-0.683\phi^{3/2} v(y)/F\right] \quad (A) \end{aligned} \qquad (3)$$

where A is the area of the emitting surface from which the collected current originates. The image correction terms t(y) and v(y) are slowly varying tabulated functions of the auxiliary variable $y = (e^3 F)^{\frac{1}{2}}/\phi$.[10]

From Eq. (1), it is apparent that $dI_c/d\varepsilon$ turns on abruptly at the emitter Fermi level when p is small and decays exponentially with decreasing electron energy. The value of the half width Δ of the TED can be obtained from Eq. (1) so that at $p = 0$, Δ is given by

$$\Delta \simeq 0.69d. \qquad (4)$$

Since the practical value of d varies from 0.1 to 0.3 eV, the experimental half widths fall in the range 0.07 to 0.2 eV.

For the retarding potential method, as diagrammed in Fig. 1, the emitted electrons can be collected at a metal surface of work function

ϕ_c only if their total energy E meets the condition

$$E > \phi_c + E_f - V_c$$

where V_c is the emitter-to-collector bias potential; thus, increasing V_c allows all electrons down to the energy level $\varepsilon = \phi_c - V_c$ to be collected at 0°K. The condition $V_c = \phi_c$ represents the current cutoff since electronic states above E_f are not populated, and the total collected current I_c at a specified value of ε is given by

$$I_c = \frac{I_o}{d} \int_0^{-\varepsilon} e^{\varepsilon/d} \, d\varepsilon = I_o (1 - e^{-\varepsilon/d}). \tag{4}$$

By rewriting Eq. (4) in the working form

$$\log_{10}(I_o - I_c)/I_o = -\phi_c/2.3d + V_c/2.3d \tag{5}$$

it is clear that the values of ϕ_c and d can be obtained from the intercept and slope respectively of a plot of $\log_{10}(I_o - I_c)/I_c$ versus V_c.

At emitter temperatures above 0°K $\log \Delta I/I_o$ versus V_c deviates from linearity due to the Boltzman distribution of electrons in states above E_f. The theoretically expected effect of temperature on the TED has been verified experimentally and is of little consequence to the accuracy of utilizing Eq. (4) to obtain ϕ_c at $T \leq 300$°K. This can be verified by noting that the temperature accounts for only a small deviation from $\ln \Delta I/I_o$ versus V_c plot near $V_c = \phi_c$ as shown in Fig. 2.

Alternatively, one may obtain ϕ_c by noting that the value of V_c

at $I_c/I_o = 0.5$ when inserted into Eq. (6) yields

$$\phi_c = V_c(\tfrac{1}{2}) - d \ln 2 \qquad (6)$$

where $V_c(\tfrac{1}{2})$ is the value of V_c for which $I_c/I_o = 0.5$. Eq. (6) is strictly applicable only for $T = 0^oK$; however, the temperature correction to $V_c(\tfrac{1}{2})$ is minor and only amounts to $\sim$ 10 meV at 300^oK. The principle sources of experimental error in this method stem from the uncertainty in the experimental values of d and I_o due to electron reflection.

Eq. (1) may be differentiated with respect to ε in order to obtain the difference ε_p in energy between the peak of the TED and the Fermi energy level:

$$\varepsilon_p = kT \ln \frac{kT}{d-kT} . \qquad (7)$$

This equation, plotted in Fig. 3 at several values of d, may be used to obtain the theoretical value of ε_p which is equal to $\phi_c - V_p$. Since V_p (the position of maximum dI_c/dV_c on the energy axis) can be obtained experimentally, the value of ϕ_c can be obtained directly from the TED curve and Fig. 3. Since in practice $\varepsilon_p \simeq 30$ mV this method gives ϕ_c easily within 1% accuracy.

Even though the assumptions of the Sommerfeld free electron model, upon which Eq. (1) and the subsequent equations are based, has recently been found to be inadequate for certain crystallographic directions of tungsten[2] and molybdenum[3], the occurrence of the emission threshold at E_f was unchanged for clean emitters. In any case,

inadequacies in Eq. (1) due to band structure effects can be easily avoided for this application by choosing an emission direction (e.g., the <111> or <310> of tungsten) for which the corresponding TED curve agrees well with Eq. (1). For that reason we have utilized for this study oriented field emitters with these directions along the emission axis. Thus, all that must be known concerning the emitter in order to apply the FERP method of work function determination is the value of d which can either be calculated with sufficient accuracy from the I(V) characteristics of the emitter or determined experimentally from Eq. (5).

ELECTRON REFLECTION

Only one property of the collector that can detract from the complete applicability of the above equations in evaluating ϕ_c is electron reflection, which cannot be eliminated by the FERP method should it occur. We can indicate the effect of reflection on Eq. (1) by noting that $I_c = I_p (1-R)$, where I_p is the primary beam current impinging on the collector, and by defining the energy dependent reflection coefficient $R(\varepsilon)$ as $R(\varepsilon) = I_r/I_p$, where I_r is the reflected current. With these definitions one may readily show that the experimentally measured quantity $dI_c/d\varepsilon$ is given by

$$dI_c/d\varepsilon = \alpha(\varepsilon)\, dI_p/d\varepsilon - I_p\, d\alpha/d\varepsilon \qquad (8)$$

where $\alpha(\varepsilon) = 1-R(\varepsilon)$ is the electron acceptance coefficient and $\varepsilon = |\phi_c - V_c|$ is the maximum kinetic energy of the collected electrons. Near the collection current threshold (i.e., $\varepsilon \sim 0$) the last term of Eq. (8) will be small compared to the first since $I_p \to 0$ as $\varepsilon \to 0$ and $d\alpha/d\varepsilon$ is normally small at $\varepsilon \to 0$.

However, as the energy of the primary electron beam increases above the threshold voltage considerable changes may occur in $\alpha(\varepsilon)$ (i.e., $d\alpha/d\varepsilon$ becomes large) which in turn will cause serious deviation in the apparent value of I_p. Thus, plotting the data according to Eq. (5) in order to obtain an accurate value of ϕ_c and d will not be possible. In like manner it will be difficult to utilize Eq. (6) in order to obtain ϕ_c due to the inability to obtain an accurate value of I_o.

In contrast, Eq. (7) is basically unaffected by reflection since the last terms of Eq. (8) can usually be neglected at $\varepsilon \simeq \varepsilon_p$. We should also point out that a cursory examination of Fig. 3 reveals that ε_p is very small (less than 40 mV) at practical values of d and T so that uncertainties in the exact position of ε_p due to reflection will not introduce appreciable error in the value of ϕ_c. Thus, in the event that detectable reflection occurs for a particular collector, the evaluation of ϕ_c should be accomplished from the TED curve through Eq. (7).

EXPERIMENTAL APPROACH

The basic requirement of the electron optical system for this application is to transform the highly diverging electron beam at the source into a co-linear beam normal to the collector substrate surface and which can be decelerated to zero volts. In order to maximize the analyzer energy resolution the electron source must be highly apertured[11] which in turn causes a very low beam transmission coefficient of the order of 10^{-3} to 10^{-4}. However, if the emitter is to be operated at room temperature the resolution of the analyzer need only to be ~ 100 mV; therefore, an electron optical system which sacrificed unnecessary resolution in order to obtain a larger collector current to speed the data acquisition was designed for this application. Rather than aperture the primary beam to the usual ~1° half angle Θ in order to maximize resolution we chose for this application $\Theta \simeq 8°$; depending on the orientation of the emitter this aperture angle allowed a beam transmission of the order of 10%. Currents in the 10^{-7} A range were easily obtained in the focused spot thereby allowing the gun to be used as an electron source for other applications as well.

The electrostatic focusing system used in the analyzer shown in Fig. 4 consists of an anode, two Einzel lenses and a 500 line/in decelerating mesh electrode which established parallel equipotential

lines in front of the collector. All electrodes were made from molybdenum. A two stage electrostatic focusing system with a virtual crossover in front of the first lens was chosen over a single stage because of its greater optical efficiency. The lens circuitry is shown in Fig. 5, and the lens operating voltages given in Table I were arrived at by analytical computer analysis and confirmed experimentally. The anode electrode controls the emission level; varying the voltages on the downstream focusing electrodes have negligible effect upon the emission current. As the beam enters the first Einzel lens it is partially decelerated and forms a virtual image of the source ~ 2 mm behind the emitter tip. The second Einzel lens focuses the virtual tip image into a ~ 0.5 mm spot size at the mesh electrode E_9. Further deceleration occurs between electrode E_8 and the mesh E_9. In most cases the mesh was operated between 5 and 10 V relative to the emitter, thereby providing a nearly field free region between the mesh and the collector at the current threshold. Examination of the spacial characteristics of the beam showed that no blow up of the beam occurred even down to the cut-off voltage of the mesh. By varying the screen voltage to lower values and measuring the transmitted current in a Faraday cage, the energy distribution curve of the electron beam passing through the mesh was found to be in agreement with the theoretical shape. Also, from the position of the current threshold the mesh work function was found to be approximately 4.6 eV.

The lens system was aligned and mounted securely on four longitudinal glass rods. Both the emitter and anode could be removed as a unit from the tubular anode holder. In this way the emitter, which was held in place by a Corning 1720 glass bead in a molybdenum tube, could be easily replaced and prealigned in the center of the 10 mil anode aperture prior to insertion into the anode holder. By positioning the emitter in the plane of the anode aperture, no interception of the primary beam occurred at the anode or subsequent elements of the first lens. Aperturing occurred in the nearly field free region of the second Einzel lens by placing two 40 mil diameter stops in the last lens tube. Thus, electron induced desorbed ions or neutrals from the anode was eliminated and the high positive potential saddle at the anode prevents ions generated beyond the first aperture from bombarding the cathode. This design feature greatly improves the current stability without requiring rigorous outgassing of the electrodes. The angular convergence of the beam at the collector was fixed by geometry to be $< 1.4^{\circ}$ for a well focused spot. Hence, negligible loss in resolution resulted from the angular deviation of the beam from perpendicularity at the collector.

The large aperture angle of the analyzer necessarily reduced the resolution of the tube as a retarding energy analyzer. Using the voltage separation between the 10 and 90% points on the leading edge of the energy distribution as described by Young and Kuyatt,[12] the re-

solution of the gun was determined as being 50 to 80 mV. This resolution was adequate to resolve the leading edge of the energy distribution curve at room temperature.

The emitter orientations selected for the field electron source in this study were <111> and <310> tungsten, fabricated from zone oriented wire. Previous studies[2] have shown that electrons field emitted from these orientations exhibit energy distribution curves that agree closely with the Sommerfeld free electron model upon which the theoretical expressions of the previous section are based. Furthermore, the work functions of the crystal planes intersecting these directions are quite low -- 4.3 eV for the (310) plane and 4.4 eV for the (111) plane -- thereby providing the highest beam transmission values.

The single crystal collector substrates of this study were shaped and mounted in the holder as shown in Fig. 4. The face of the collector crystal was circular with a diameter of 200 mils. This was sufficiently large compared to the 20 to 40 mil beam size to eliminate edge effects. Thermal cleaning of the collector crystal was accomplished through electron bombardment. Collector crystals could be easily replaced by removing the glass seal which holds the collector support rod.

EXPERIMENTAL PROCEDURE

The single crystal collector surfaces were fabricated from MARZ grade material by a high speed grinding wheel and electrochemical machining techniques. Several mils of the collector surface were removed by electrochemical etching in order to eliminate mechanical defects. The etchant solutions for the copper, tungsten, and iridium surfaces were concentrated phosphoric, sodium hydroxide, and 5% sodium hypochlorite, respectively. The alignment of the desired crystal directions with respect to target normal was within $\pm 1^{\circ}$ as shown by Laue x-ray examination. Monocrystallinity of the substrates were carefully checked by a high powered optical microscope.

After mounting the collector substrate, the tube was evacuated to $\sim 10^{-10}$ torr pressure range. The arrangement allowed for the option of immersing the tube partially or completely in liquid nitrogen in order to enhance vacuum stability and to extend the temperature range of the work function measurements.

Cleaning of the crystal surface was accomplished by electron bombardment heating to 2000° and 1700°K in the case of tungsten and iridium, respectively. The copper crystal was exposed to 10^{-6} torr of hydrogen and heated to 1250°K. Thermal heating was con-

tinued until the field electron emitter, which was also cleaned thermally, and therefore very sensitive to gas phase contamination, showed no change in work function after flashing the collector substrate to its cleaning temperature. As a corollary check, the absence of further change in the collector work function on heating was used as an indication of a clean surface.

The emitter-to-collector current-voltage characteristics were taken several times for each collector crystal and plotted on an x-y recorder. A computer program was formulated to plot the data according to Eq. (5) so that a value of ϕ_c and d could be obtained. As will be noted later in the paper this method of determining ϕ_c and d was not always applicable due to reflection. Therefore, the differential curve was also taken by utilizing the position 3 circuitry shown in Fig. 5, which involves the well known electronic differentiation method utilizing a PAR HR-8 Lock-in Amplifier. A 10 mV 1000 hrz signal v_s was fed to the emitter through the transformer T_3. The magnitude of this signal detected by the Lock-in Amplifier (LA) is proportional to dI_c/dV. From the position of the TED peak and Eq. (7), a value of ϕ_c could be obtained; this could be accomplished with an experimental accuracy of ± 20 mV. The I-V and TED data were usually taken at emitter temperatures of 77 and 300°K.

EXPERIMENTAL RESULTS

Three new values of ϕ_c obtained by the FERP method are reported in Table II along with previously determined values for other collector surfaces. The new values reported here for Cu(100), W(111) and Ir(111) were obtained through Eq. (7) from the TED curves shown in Fig. 6. An interesting feature of these results is the additional structure in the TED for Cu(100). This anomalous structure near threshold in the TED curve was not apparent in the W(111) and Ir(111) results and was determined to be a function of the collector type. The integral current-voltage characteristics shown in Figs. 7-9 on a contracted voltage scale clearly shows that the origin of the TED structure in Cu is clearly due to reflection at the collector surface which varies rapidly at the threshold voltage.

If we assume that all the reflected electrons are collected at the mesh the sum of the collector current I_c and mesh current I_s is given by

$$I_p = I_c + I_s \tag{9}$$

where I_p is the emitter current arriving at the mesh and I_p' is the current impinging on the collector. Noting that the mesh transmission is given by $I_p'/I_p = T$ and that $(1-R) = I_c/I_p'$, one obtains

$$(1-R) = I_c/T\,(I_c + I_s). \tag{10}$$

Since T, I_c and I_s are measurable quantities R may be determined as a function of V_c as shown in Figs. 7-9 for each of the substrates. It is important to point out that Eq. (10) is valid when I_p' is at its saturated value. Since we wish not to count electrons reflected by the retarding field, it is necessary to use the theoretical variation of I_p' with V_c to calculate R in the deep retarding range. The theoretical dependence of the current I_p' on V_c is also plotted in Figs. 7-9 with appropriate normalization factors applied. Only in the case of Cu is there some uncertainty about the value of I_s and hence the absolute value of R. Clearly the values of R for both Ir(111) and Cu(100) are unusually high near threshold and exhibit considerable structure. It must be remembered that the energy spread of the primary beam is $\approx$ 0.2 eV so that values of R within $\approx$ 1 V of threshold should be viewed as integral values rather than mono energetic values. However, with these definitions in mind, one may confidently measure R down to zero primary beam energy. It should be pointed out that in order to obtain the value of primary beam energy in Figs. 7-9 the respective values of ϕ_c must be subtracted from the abscissa.

In our experimental setup when $V_c - \phi_c > V_s - \phi_s$ (s refers to the screen-mesh electrode) those reflected electrons which lose energy through inelastic processes will not be collected at the mesh but rather returned to the collector. In view of the fact that the inelastically reflected component is negligible for most substrates near

zero beam energy, our value of R for the most part pertains to elastically reflected electrons when $V_s \simeq 5 - 10$ V. This condition was true for the Ir results. However, for the W(111) and Cu(100) reflection data V_s was 130 V; thus, R values in these cases refer to elastically and inelastically reflected electrons. Experimentally, it was found that the inelastically reflected electrons were a sufficiently small part that they has very little effect on the overall structure of the R vs V_c curves.

DISCUSSION

The work function value reported here for the W(111) plane is in close agreement with values reported by other methods, particularly thermionic and field emission methods. Since the reflection coefficient is low (less than 15%) near threshold, the value of ϕ_c obtained from Eq. (5) compares within experimental error with the value computed from the TED, Eq. (7). This merely provides the expected self consistent check on the experimental technique when reflection is small or unchanging with primary beam energy near the threshold. The value of R and its variation with beam energy is almost identical to careful reflection studies with a highly monoenergetic (100 mV beam spread) electron gun used by Armstrong.[13] Even the small peak at 10.3 V in the Fig. 7 reflection curve was also observed by Armstrong,

thus showing the high degree of sensitivity and correlation of the two methods. Also, as shown by Armstrong, surface contamination markedly alters reflection curves; thus, the close argument in shape of the R vs V_c curve mutually supports the claim of atomically clean surfaces for these results.

Because of our ability to accurately measure R to within a few tenths volt of threshold our results show structure heretofore unobserved in the form of a definite peak in R(111) at 7.5 - 4.4 = 3.1 V and a minimum at 5.0 - 4.4 = 0.6 V beam energy.

The work function value of 5.1 eV measured for Cu(100) by the FERP method is close to the 4.9 eV value measured by thermionic methods.[14] Undoubtedly, surface contamination due to bulk impurities or surface oxide layers can easily plague copper work function values. We believe, however, that our value represents a near clean value since heating in hydrogen followed by heating in vacuum gave a reproducible result for ϕ_c. We note further that the theoretical value of ϕ_c for Cu(100) obtained from a semi-emperical theory by Steiner and Gyftopoulos[15] agrees closely with the value reported in this study.

Due to experimental difficulties the value of R was not measured for Cu(100) over as large a range as W(111); yet the results in Fig. 8 show an unusual large variation of R with beam energy near threshold. A very large maximum (~ 50%) in R occurs near threshold followed

by smaller peaks at 0.8 and 2.0 V and a low value (< 5%) at 3.0 V above threshold. The relative magnitude of the peaks was altered by surface contamination; however, the position of the peaks was unchanged.

Measurements of the elastically reflected 00 beam through the variation in LEED spot intensities have also revealed a large value of R near the threshold beam voltage.[16] This can be understood from the electron energy band calculation for copper along Γ x by Burdick.[17] It is shown that a complete band gap occurs around the vacuum level so that electrons of this energy are strongly forbidden inside the crystal and hence reflected. The fine structure in R between threshold and 3 V has not been observed previously and probably arises from details of the reflection occuring near the band edges. If the decrease in R near threshold represents the bottom edge of the band gap the energy gap appears to be roughly 1.5 to 2.0 V.

The work function for Ir(111) of 5.76 eV is one of the highest values reported in the literature for a clean macroscopic surface. LEED studies of the (100) face of Ir[18] indicate that the surface is stable with respect to thermal heating and shows no tendency to facet as does the high work function (0001) plane of Re.[19]

Another interesting feature of the Ir(111) work function was the observation that residual gas adsorption lowered the work functions. This was contrary to the work function change observed on most

other crystal surfaces studied.

Perhaps the most spectacular result of this report is the extremely large value of R at threshold for Ir(111) -- nearly 80%. This result was very reproducible and must be carefully considered when retarding potential measurements are being performed on this crystal face. We have not yet obtained information on the electronic band structure for Ir so that we cannot say for sure that the large value of R is due to a band gap as was the case for Cu(100).

SUMMARY

The values of work function for W(111), Cu(100) and Ir(111) have been measured and agree closely with predicted values obtained from semi-empirical models. A very high work function of 5.76 eV was observed for Ir(111). Electron reflection coefficients were also obtained for each crystal face. Both Cu(100) and Ir(111) exhibit unusually large values of R near the threshold voltage. The large value of ϕ for Ir(111) makes it an interesting candidate as a collector surface for a thermionic converter. However, studies of Cs adsorption on Ir(111) must be completed in order to verify this possibility. Also, the large bare surface electron reflectivity, which is an undesirable feature for an efficient electron collector surface, must be measured with adsorbed Cs in order to fully evaluate its usefulness in thermionics.

Table I. Operating voltages on lens elements (see Fig. 3) with emitter at 0 V.

Lens element	Operating voltage
E_4	$0.06E_3$
$E_5=E_7$	0
$E_6=E_8$	$0.04E_3$
E_9	5-10 or 130-150 V

Table II. Work function values at room temperature.

Material	ϕ_c	ϕ (predicted)*
W(110)	5.25 ± .02 eV	5.50
W(100)	4.63 ± .02	4.66
W(111)	4.47 ± .03	4.47
Nb(100)	4.18 ± .02	4.08
Ni(100)	5.53 ± .05	5.20
Cu(100)	5.10 ± .05	4.99
Ir(111)	5.76 ± .04	5.56
Re(0001)	5.34 ± .05	5.53

* by a semi-empirical method of Steiner and Gyftopoulos[15]

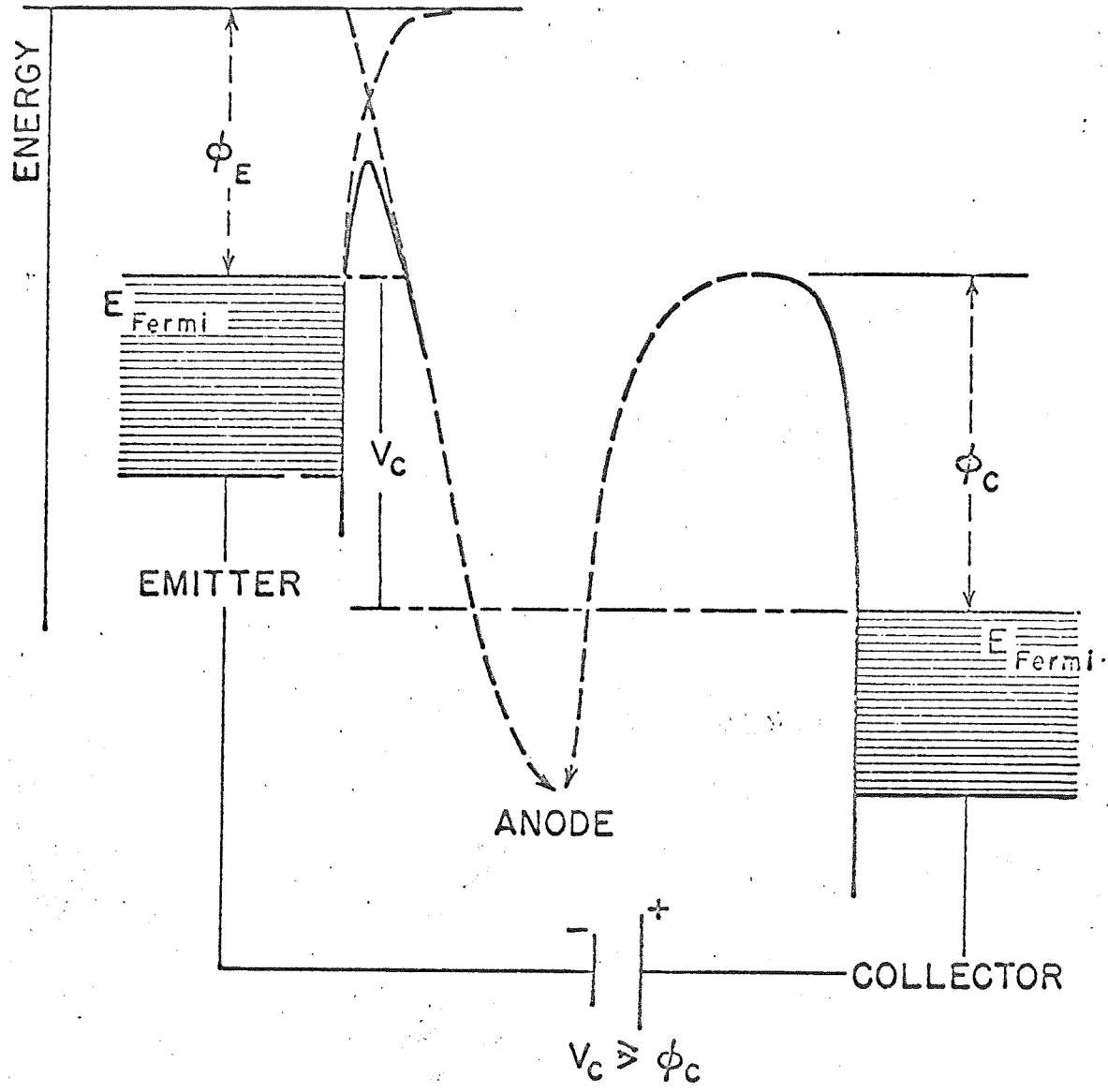

Figure 1. Potential energy diagram for field emission retarding potential measurements. When the collector is biased such that only electrons from the fermi level of the emitter can reach the collector, the battery voltage V_c is equal to the collector work function ϕ_c.

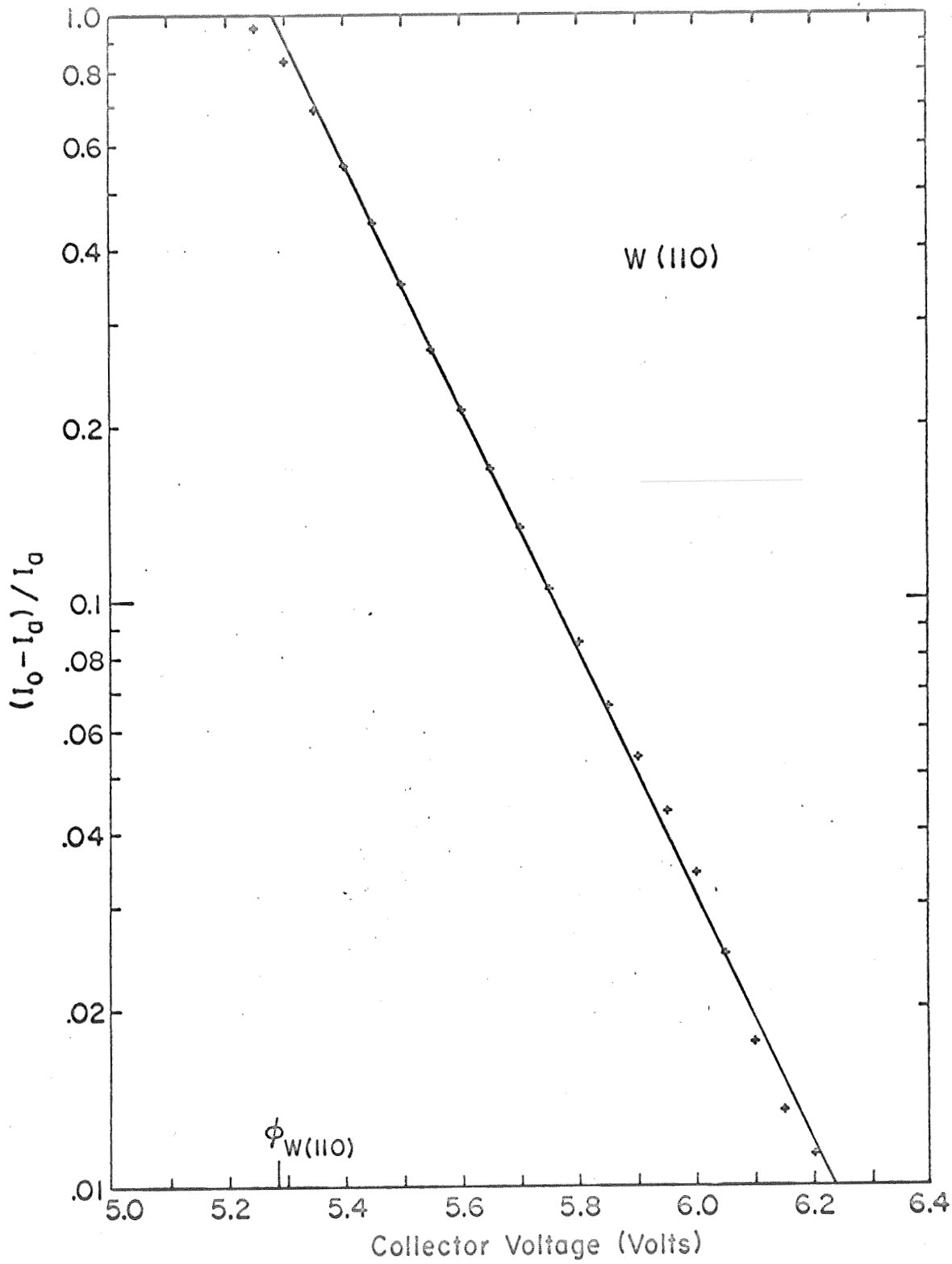

Figure 2. Plot of ln $\Delta I/I_o$ vs bias voltage for a W(110) collector. The intercept of the abscissa at $\Delta I/I_o = 1$ give ϕ according to eq. (5).

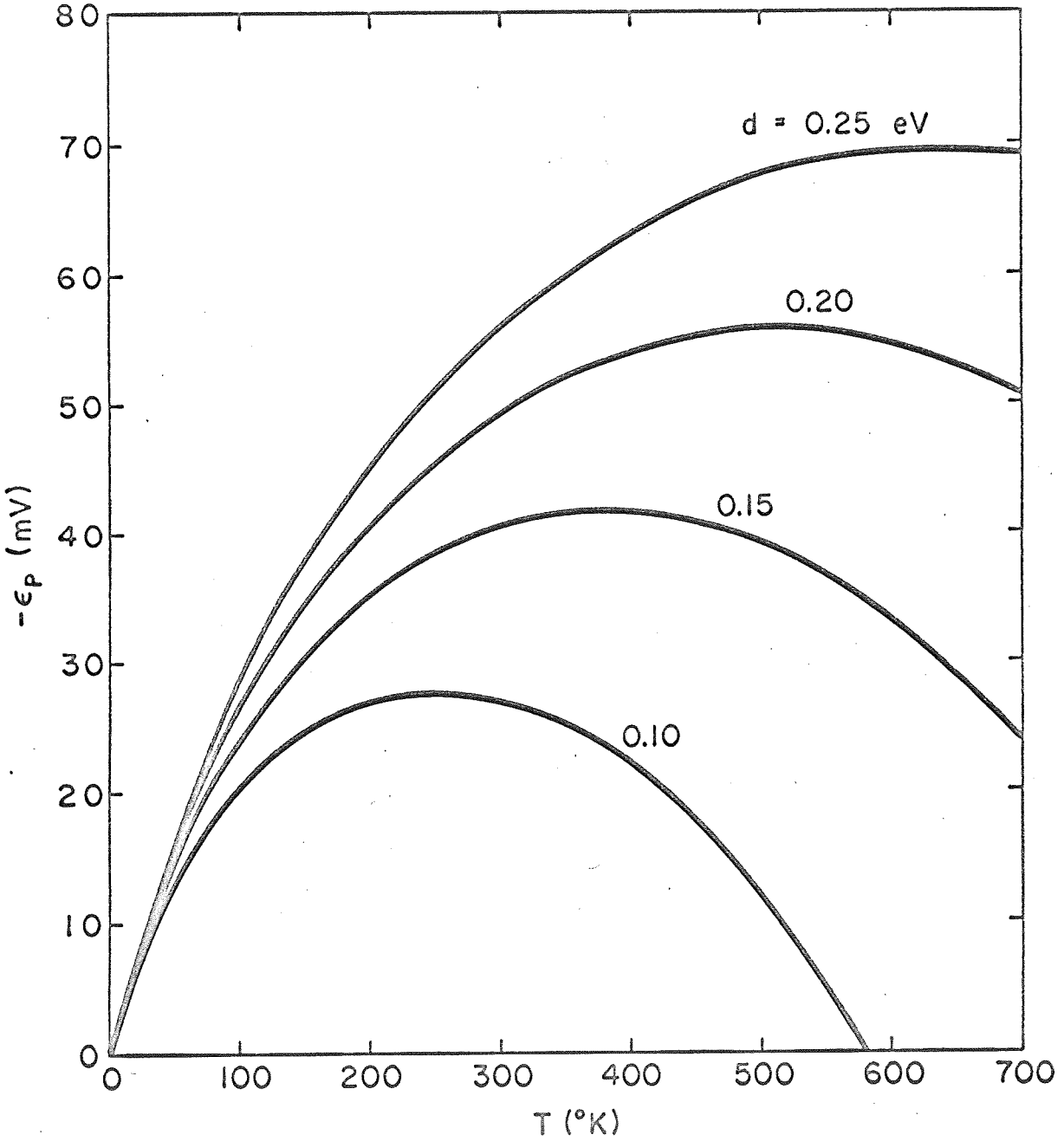

Figure 3. The difference ϵ_p in energy between the peak of the total energy distribution curve and the Fermi energy level as a function of temperature T and energy parameter d.

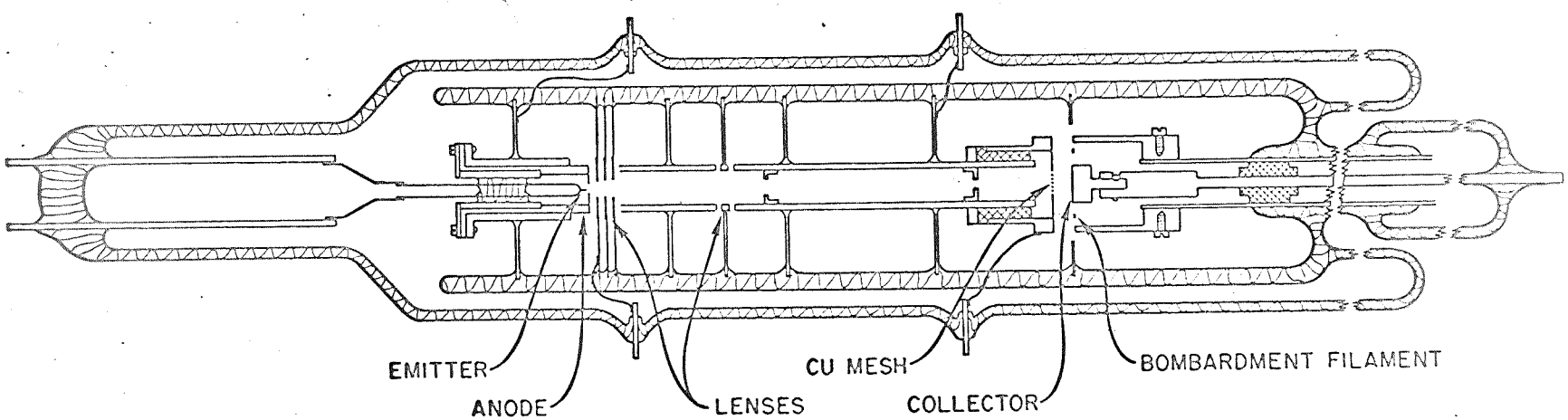

Figure 4. Diagram of the FERP tube showing the pertinent features of the optical system and collector.

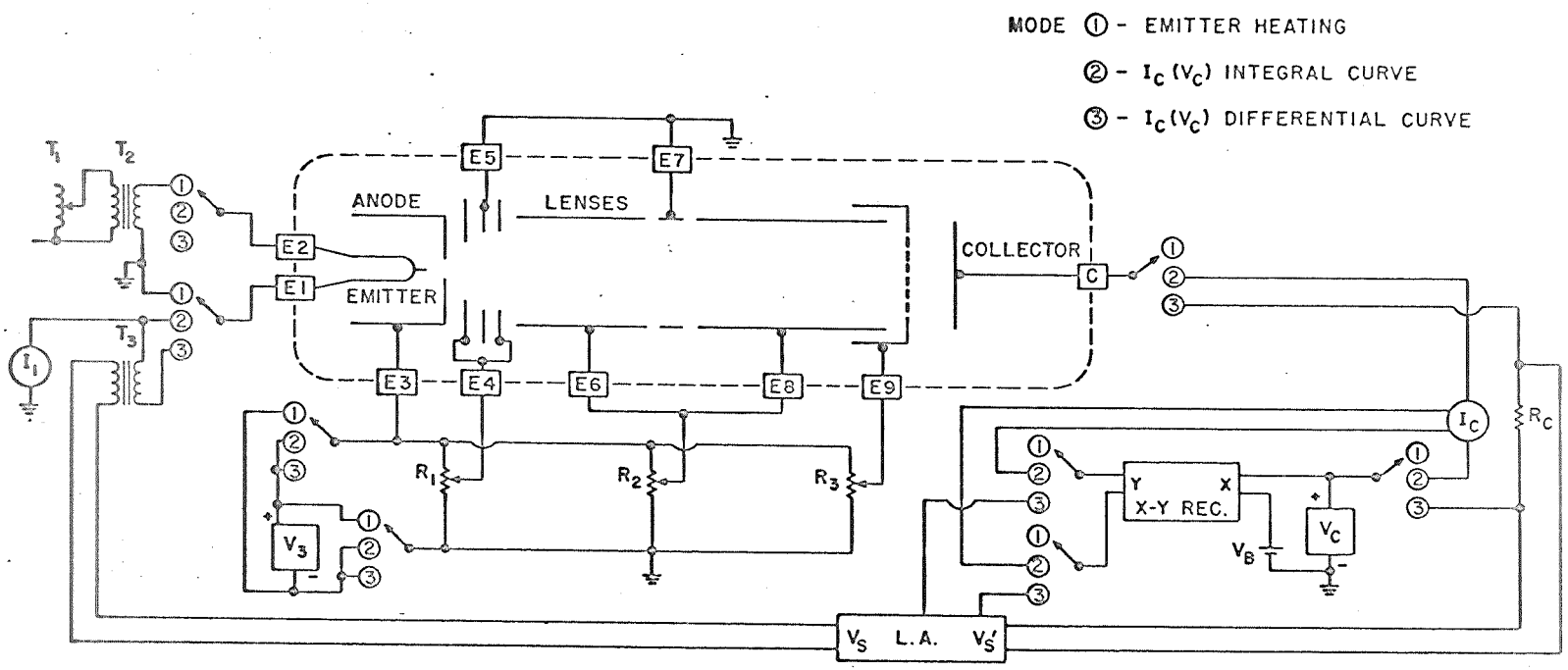

Figure 5. Diagram of the electrical circuitry associated with the FERP tube.

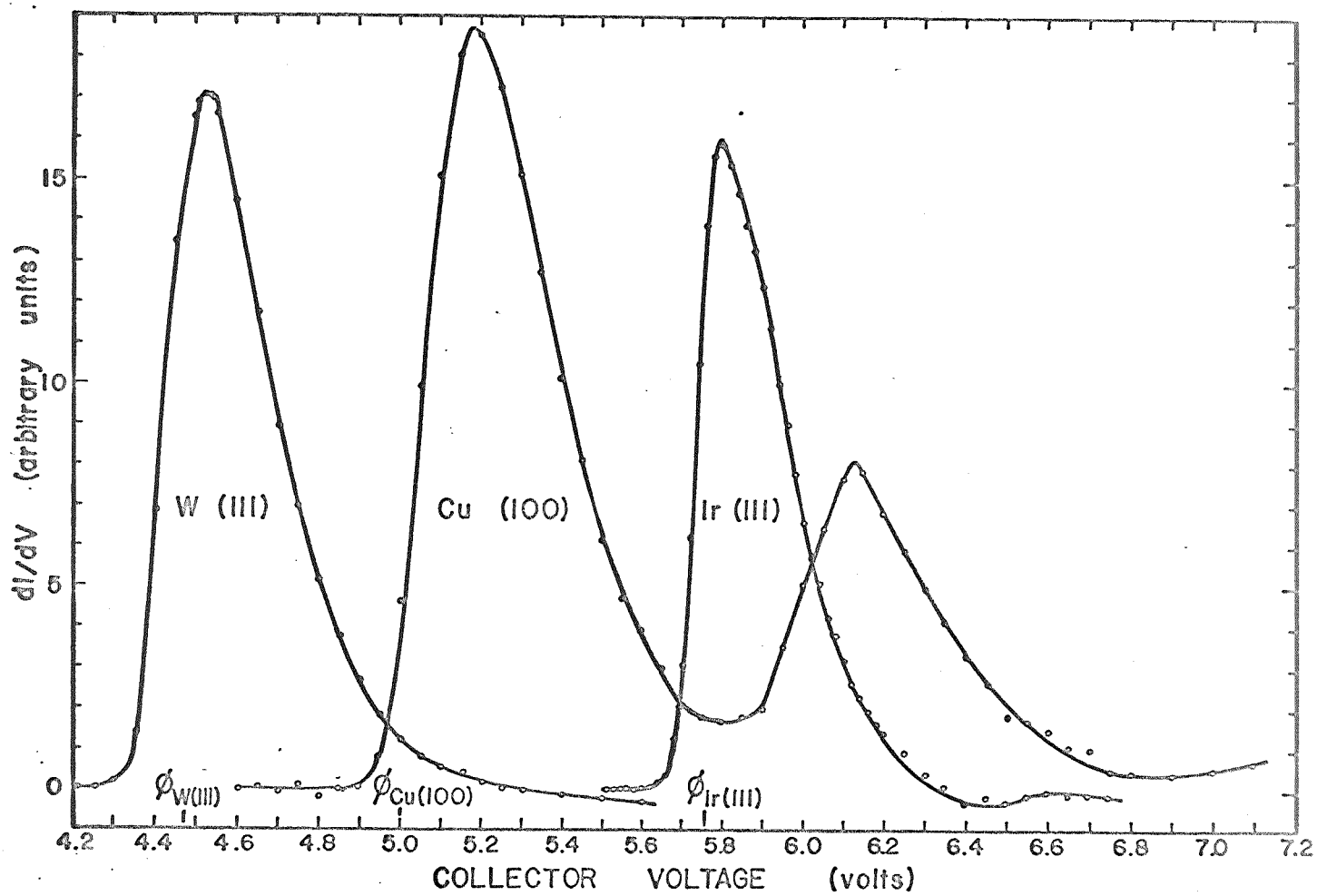

Figure 6. TED curbes for W(111), Cu(100) and Ir(111) obtained from the FERP tube.

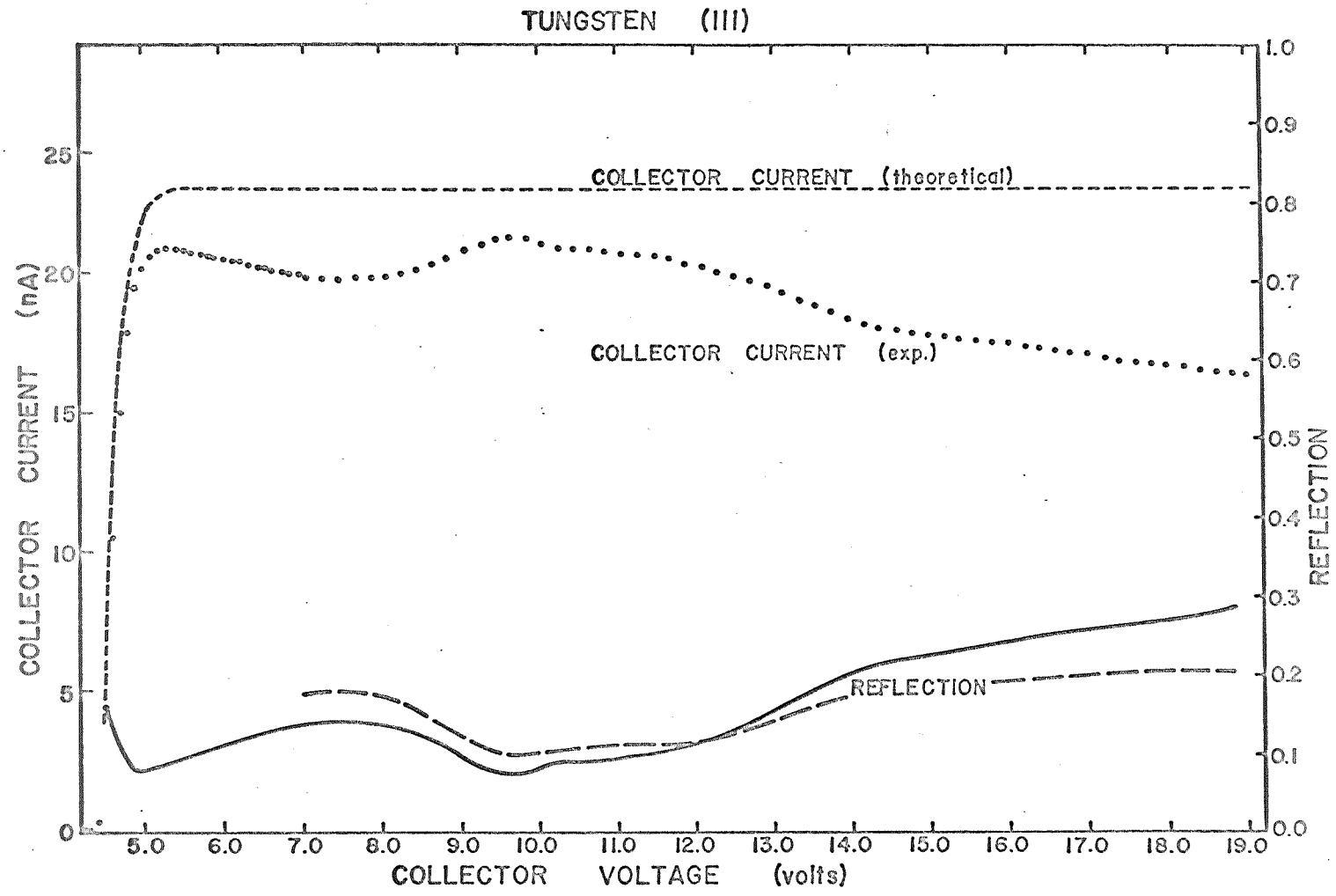

Figure 7. Experimental and theoretical integral current-voltage curves obtained for W(111). Solid line shows the experimental reflection coefficient computed from eq. (10). Dashed curve shows the experimental reflection curve obtained by Armstrong[13] by other techniques.

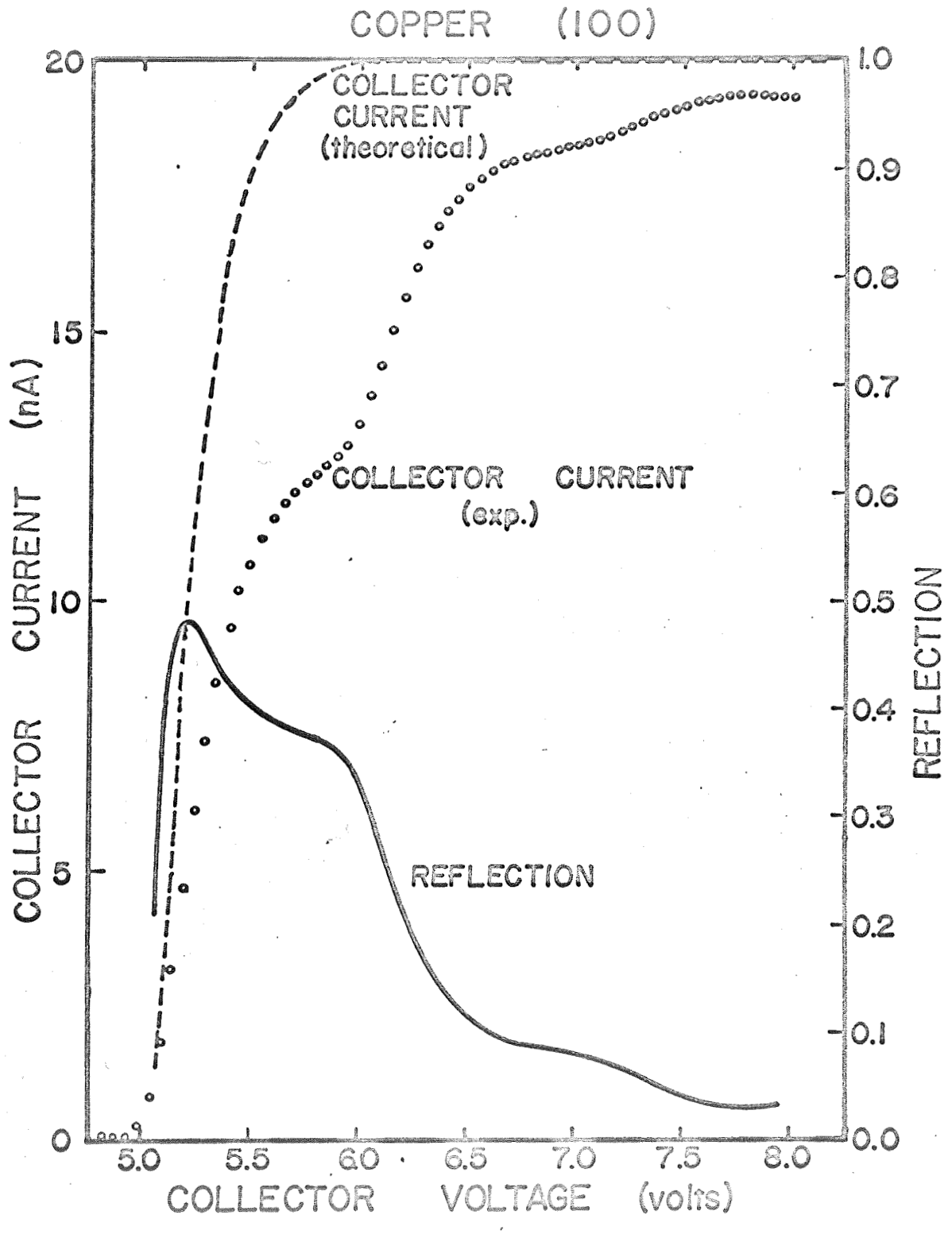

Figure 8. Experimental and theoretical integral current-voltage curves obtained for Cu(100). Solid line shows the experimental reflection curve.

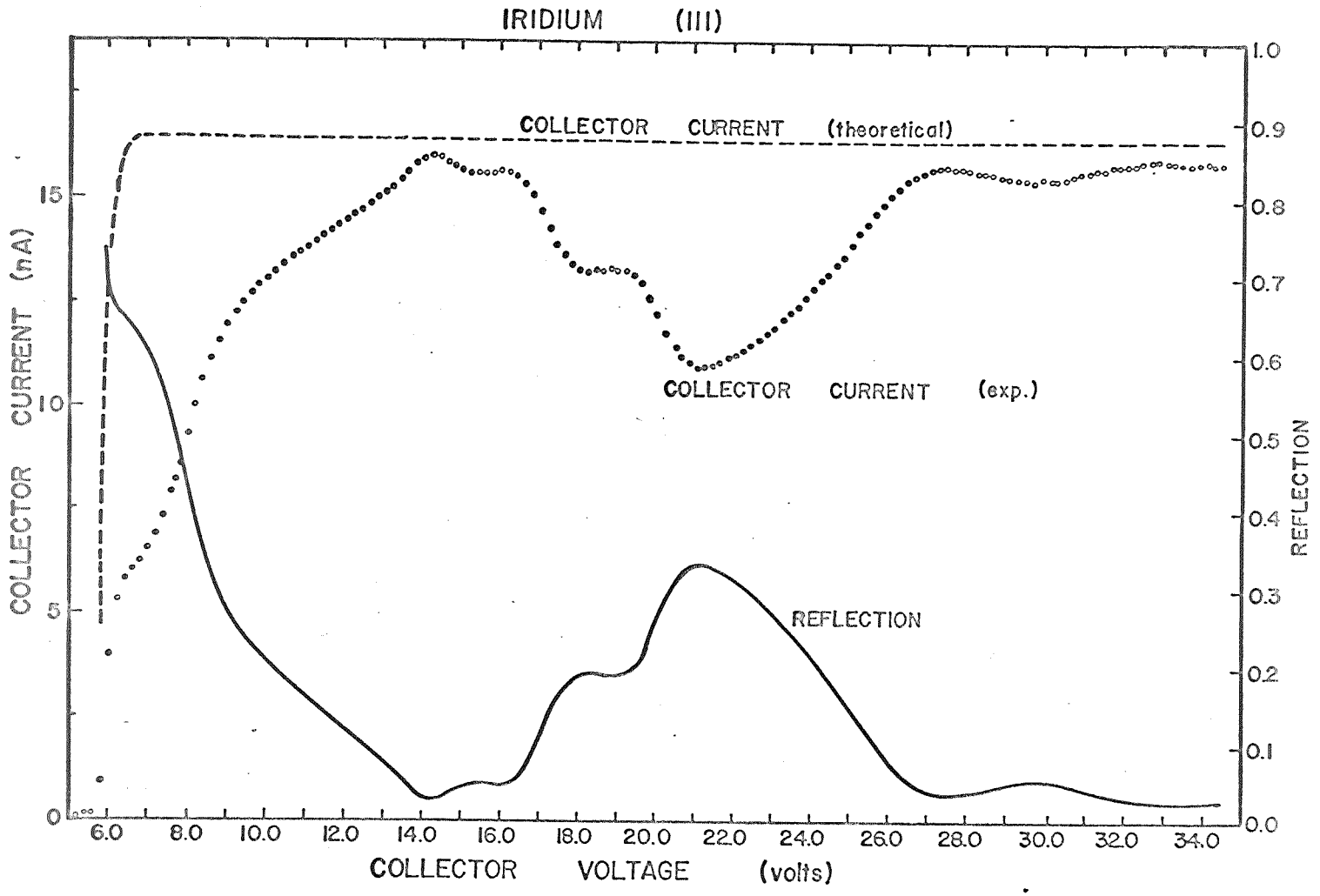

Figure 9. Experimental and theoretical integral current-voltage curves obtained for Ir(111). Solid line shows the experimental reflection curve.

REFERENCES

1. F.I. Itskovich, Soviet Physics JETP 23, 945, 1425 (1966); 24, 202 (1967).

2. L.W. Swanson and L.C. Crouser, Phys. Rev. 163, 662 (1967).

3. L.W. Swanson and L.C. Crouser, Phys. Rev. Letters 19, 1179 (1967).

4. R.D. Whitcutt and B.H. Blott, Phys. Rev. Letters 23, 639 (1969).

5. J.E. Henderson and R.E. Badgley, Phys. Rev. 38, 590 (1931).

6. A.A. Holscher, Surface Sci. 4, 89 (1966).

7. H. Shelton, Phys. Rev. 107, 1553 (1957).

8. R.D. Young and E.W. Müller, Phys. Rev. 113, 114 (1959).

9. A. van Oostrom, Phillips Res. Rept. Supp. (Netherlands) 11, 102ff (1966).

10. R.H. Good and E.W. Müller, Handbuch der Physik, edited by S. Flügge (Springer-Verlag, Berlin, 1956), Vol. 21, p. 176.

11. T.E. Everhart, J. Appl. Phys. 38, 4944 (1967).

12. R.D. Young and C.E. Kuyatt, Rev. Sci. Inst. 39, 1477 (1968).

13. R.A. Armstrong, Can. J. Physics 44, 1753 (1966).

14. E.H. Blevis and C.B. Crowell, Phys. Rev. 133A, 580 (1964).

15. D. Steiner and E.P. Gyftopoulos, Proceedings of the 27th Annual Conference on Physical Electronics, March 1967, Mass. Institute of Technology.

16. S. Anderson, Surface Sci. 18, 325 (1969).

17. G.A. Burdick, Phys. Rev. 129, 138 (1963).

18. J.T. Grant, Surface Sci. 18, 228 (1969).

19. L.G. Feinstein and M.S. Macrakis, Surface Sci. 18, 277 (1969).

II

Cesium Adsorption-Desorption Characteristics on W(110)

INTRODUCTION

Although Cs adsorption-desorption on W is a much studied system by a variety of methods there still exists little reliable thermal desorption and sticking coefficient data on macroscopic single crystal faces. In addition, considerable discrepancy exists with respect to the absolute adsorbed atom density scale as a function of work function change. For example, one study[1] gives 1.5×10^{14} atoms/cm^2 as the coverage at the minimum work function for W(110), while other studies give 3.2×10^{14} atoms/cm^2 and 3.5×10^{14} atoms/cm^2 as the correct values.[2,3] In order to resolve some of these apparent conflicts in the literature and to give more precise and unambiguous data from which relationships among work function, coverage and temperature can be obtained, we have set forth to develop a simple, but effective method of securing the needed data.

In this section we shall describe an extension of the field emission detection method developed by Bell and Gomer[4] of measuring sticking coefficients of Cs ions and neutrals and thermal desorption rates in various known coverage intervals. Because of the small size of the field emitter detector and its high sensitivity, a very small

portion of the center of a macroscopic crystal face can be sampled and thereby reduce undesirable edge effects. Also the undesirable effect of concomitant backside surface diffusion, which confuses desorption measurements when large area detectors are employed, is reduced and can be evaluated by this method. At present our results are confined to W(110), but will be extended to other substrates of interest as thermionic converter electrodes.

METHOD OF APPROACH

A diagram of the experimental tube is given in Fig. 1. The Cs source consists of a reservoir from which Cs can be condensed onto a resistively heatable Pt disc. By immersing the entire tube in liquid nitrogen the Cs vapor pressure is negligible. By use of an accurate heating circuit a controlled amount of Cs can be deposited onto the single crystal target which, in this case, consists of a circular disc 0.125" in diameter and 0.015" thick. The target surface was smoothed by electrical chemical machine etching. The target crystal could also be heated in a controlled fashion by the usual 4 wire resistive heating and potential sampling techniques. Temperature measurements were accomplished by utilizing the relation between the resistivity change and temperature. For the most part temperatures were below the point where radiative corrections were necessary and pyrometric measurements showed less than a 10^{o} variation across the crystal at 1200^{o}K.

A field emitter mounted on a slide assembly could be positioned directly in front of the target crystal by relaxing the current through

the external magnet. In the down position the tip was approximately 0.050" from the center of the target crystal.

The desorption of Cs or other adsorbates could be sensitively measured by noting the change in the work function of the emitter through the field emission current-voltage relationships. The I(V) data was taken with the emitter in the "up" position thereby allowing the field emission pattern to be displayed on the phosphor screen. In order to determine the amount of Cs on the emitter a relationship between emitter work function and Cs coverage must first be established. As alluded to previously some disagreement exists as to the correct work function-coverage relationship for Cs on W. In this work we employed the relationship determined previously in this laboratory[1] and which, as shown in the following section, was verified by this work.

In order to relate the coverage in atoms/cm^2 on the emitter to the amount desorbed from the target the following assumption was made. If isotropic desorption is assumed (i.e., all directions within a solid angle $\Omega_o = 2\pi$ are equally probable), then the ratio of the emitter coverage σ_e to target coverage σ_t is

$$\sigma_e/\sigma_t = \frac{1}{\Omega_o}\int_0^{\Omega} d\Omega. \qquad (1)$$

Letting R equal the tip to target distance and ρ_o equal the target diameter, Eq. (1) can be solved to give

$$\sigma_e/\sigma_t = 1/2 \ln \frac{[\rho^2_o + R^2]}{R^2} \qquad (2)$$

Since $\rho_o = 0.125''$ and $R = .050''$ we obtain

$$\sigma_e / \sigma_t = 0.9905.$$

Sensitivity

One of the important advantages of this method is its extreme sensitivity of detection. The field emission current I is related to work function ϕ and field strength F by the well known Fowler-Nordheim equation

$$I \simeq 1.54 \times 10^{10} AF^2 \exp(-0.68\, \phi^{3/2}/F) \quad (A) \qquad (3)$$

where A is the emitting area and F and ϕ are in units of $V/\mathring{A}$ and eV, respectively. One can easily show that

$$\frac{dI}{I} = \frac{1.02\, \phi^{3/2}}{F} \frac{d\phi}{\phi}. \qquad (4)$$

Furthermore, since the fractional monolayer coverage is a linear function of ϕ at low coverage, one may rewrite Eq. (4) as

$$\frac{dI}{I} = \frac{1.02\, \phi^{3/2} b}{F} \frac{dN}{N_o}. \qquad (5)$$

where N_o is the monolayer adsorbate density and $b = 2\pi\mu N_o$. The adsorbate dipole moment μ directly controls the sensitivity of dI/I with dN/N_o. For Cs on W, b is the order of 10 eV and $\phi^{1/2}/F \sim 7$ for typical emission levels; thus

$$\frac{dI}{I} \simeq 7b\frac{dN}{N_o} \simeq 70\frac{dN}{N_o}.$$

Assuming a 1% change in current is measurable, we find that $dN/N_o \simeq$

1.4×10^{-4}. Since according to Eq. (2) $\sigma_e / \sigma_t \simeq 1$, it follows that the sensitivity of the field emission detector to a coverage change on the target is roughly 140 parts per million. This is nearly single atom sensitivity! For electro-negative adsorbates where b is smaller the sensitivity is reduced; however, even for b ≃ 1 eV, $dN/N_o \simeq 1.4 \times 10^{-3}$ which is still the order of 0.1% coverage change sensitivity. Thus we conclude that this approach is an extremely sensitive method of measuring desorption rates or sticking coefficients.

EXPERIMENTAL PROCEDURES

One of the problems that must be carefully considered in establishing the accuracy of this method of measuring desorption rates is that of surface diffusion to the back side of the crystal simultanious with thermal desorption. This problem can be put into focus by noting that the average distance $\langle x \rangle$ an adsorbed atom diffuses before desorbing is given by

$$\langle x \rangle = (D\tau_a)^{1/2} \tag{6}$$

where D is the surface diffusion coefficient and τ_a is the life time of the adsorbed atom with respect to desorption. Noting that

$$\tau_a = \tau_{oa} e^{E_a/kT} \tag{7}$$

and that

$$D = \frac{a_o^2}{\tau_{od}} e^{-E_d/kT} \tag{8}$$

and combining with Eq. (6), we find that

$$\langle x \rangle = a e^{(E_a - E_d)/2kT} \tag{9}$$

where a is the diffusion hop distance and E_a and E_d are the activation energies for desorption and diffusion respectively. In deriving Eq. (9) we assume that the frequency factors for desorption τ_{oa}^{-1} and diffusion τ_{od}^{-1} are equal.

In order that diffusion not be a factor in perturbing the desorption rate the value of $\langle x \rangle$ must be small (i.e., less than the crystal dimensions) and/or the detector must sample a region small compared to $\langle x \rangle$. Since in practice $T \propto E_a$, the value of $\langle x \rangle$ remains sufficiently small, even though E_a increases with decreasing coverage. In order to verify this experimentally the following procedure was carried out.

A known amount of Cs (approximately 2 monolayers coverage) was deposited onto the target. The Cs source flux was determined by heating the W(110) target so that all of the impinging Cs was surface ionized and the current measured. After a total flux of 6.85×10^{14} atom/cm^2 was deposited at 77°K on the W(110) surface, a step-wise desorption of increasing temperature increments of $\sim 50^{\circ}$ was carried out with the amount desorbed measured after each desorption period of ~10 sec. If, in this process, Cs diffused around to the back side of the crystal, the total amount desorbed would not equal the amount originally adsorbed. The results of this experiment showed that the amount desorbed in this fashion equaled the amount adsorbed to within 1%. Thus, backside surface diffusion has negligible effect on the measured desorption rates.

EXPERIMENTAL RESULTS

Sticking Coefficient Measurements

By placing the tip in the down position during adsorption the only Cs that can reach the emitter tip is that which is reflected from the substrate. The following procedure was used in measuring the sticking coefficient as a function of substrate temperature and Cs coverage: (1) the substrate was brought to a specified temperature; (2) a small measured dose of Cs was deposited onto the substrate with the emitter tip in the down position; (3) the emitter was then raised to the up position and the I(V) characteristics measured; (4) the emitter was flashed clean, placed in the down position and steps (2) to (4) repeated until a monolayer or more of Cs was deposited onto the substrate.

We have carried out the above procedure for the substrate at 77°K and found that the sticking coefficient was essentially unity out to 2 monolayers coverage of Cs. Additional measurements of the sticking coefficient at higher temperatures will be performed. Also by using a Cs^+ source one may use this technique to measure sticking coefficients of ions as a function of energy.

Absolute Cs Coverage Measurements

By using a calibrated flux of Cs, it was possible to deposit a known amount of Cs on the crystal and flash it off with the tip in the down position. The amount of Cs on the tip was determined from the previously measured $\phi - \sigma$ relationship.[1] By repeating the above procedures with various sized deposits, it was found that a dose

size of $\sigma_t = 1.9 \times 10^{14}$ atoms/cm^2 on the target produced the minimum work function on the emitter. Thus, the ϕ-σ relationship determined previously[1] on the field emitter, which also showed a minimum work function at 1.9×10^{14} atoms/cm^2, was confirmed by this result.

Desorption Measurements

The desorption spectrum of Cs from W(110) was measured in the following fashion. The emitter detector was held at 100 V positive with respect to the crystal to insure that only Cs neutrals were measured at the emitter. After depositing a large dose of Cs onto the crystal (ca 2 monolayers), the substrate was heated for 10 sec intervals with the emitter detector in the down position. After each heating, the amount of Cs desorbed was measured and the process repeated at an increased temperature. Fig. 2 shows the amount of Cs desorbed as a function of temperature where $\sim 50^\circ$ temperature intervals were employed. Fig. 3 is a plot of the amount remaining on the W(110) surface after heating to a given temperature. It is interesting to note that the minimum work function, which occurs at 1.9×10^{14} atoms/cm^2 is reached at 325°K. Most evidence[1] points to a value of $\sigma = 2.8 \times 10^{14}$ atoms/cm^2 for the monolayer coverage. Thus, a portion of the monolayer Cs as well as second layer Cs appears to be desorbed in the low temperature peak around 300°K.

It is possible to measure ion desorption rates by removing the substrate-to-detector bias and thereby allowing both neutral and ionic

species to be measured. The neutral desorption rates (or amounts) can be subtracted to yield ionic desorption rates.

DISCUSSION OF RESULTS

It has been believed for some time that the sticking coefficient for Cs on W at low temperatures is unity. In this context the sticking coefficient α is defined as

$$\alpha_s = 1 - \frac{n_r}{n_o} \tag{10}$$

where n_r is the number of reflected and n_o the number of deposited atoms. The accomodation coefficient α_a, which measures the efficiency of the energy transfer, is usually defined as

$$\alpha_a = \frac{E_r - E_i}{E_s - E_i} \tag{11}$$

where E_i, E_r, and E_s are the energies of the incident, reflected, and surface atoms, respectively. It follows that if $\alpha_s = 1$, then α_a must also be unity. Straightforward application of energy and momentum conservation laws yields

$$\alpha_a = 2mM/(m+M)^2 \tag{12}$$

where m and M are the masses of the two collision partners free to move independently. From this over-simplified model, we expect large values of α where the masses of the impinging particle and substrate atoms are equal. For Cs and W we obtain from Eq. (12) that

$\alpha_a = .49$. Undoubtedly the large binding energy at low coverage and the fairly good mass match combine to give the large value of α_s observed experimentally.

Because of the extreme sensitivity of this method we can confidently claim that $\alpha = 1.0000$ for Cs on W(110) from zero to multilayer coverage. We may therefore conclude that the self condensation coefficient for Cs must also be near unity at 77°K. This experimental result is gratifying since it supports the assumption of $\alpha = 1$ used in reference 1 to calculate the experimental σ vs ϕ relationship.

Further work will establish the value of α_s as a function of σ at elevated temperatures. Obviously as T increases, at some value of σ, the apparent sticking coefficient will approach zero due to concomitant thermal desorption. Under such conditions a steady state coverage can be measured such that

$$\alpha \frac{d\sigma}{dt} = \nu\sigma \quad \exp(-E_a/kT) \tag{13}$$

where the left side is the rate of adsorption and ν is a frequency factor of the order of 10^{12}sec^{-1}. It is possible to use Eq. (13) to calculate the steady-state activation energy for desorption E_a.

By letting $d\sigma/dt$ equal the rate of coverage change during desorption, Eq. (13) can be integrated to give

$$\ln \frac{\sigma_i}{\sigma_f} = \nu t \exp(-E_a/kT) \tag{14}$$

where σ_i and σ_f are the initial and final coverages due to desorption

in time t. Using the data of Figs. 2 and 3, it was possible to evaluate E_a as a function of σ provided a value of ν was assumed ($\nu \equiv 10^{12} sec^{-1}$). The results of this calculation are shown in Fig. 4 where the horizontal bars represent the coverage increment. A comparison is given between the E_a vs σ curves for W(110) and the poly crystal results obtained elsewhere.[5] The flat portion between 1.6 and 4.0×10^{14} atoms/cm^2 is apparently due to the emptying of the loose bound state consisting of second layer and partial first layer Cs. Another less perceptible plateau, which occurs at $\sigma = 0.9 \times 10^{14}$ atoms/cm^2, appears to be another somewhat less distinct adsorption state whose binding energy is less well defined than the higher coverage binding state. The binding energy of this state appears to decrease monotonically with Cs coverage and as σ approaches zero, the value of E_a increases above 2.8 eV.

In future work the binding energy E_a of the low energy binding state as well as the higher energy binding state may be determined more precisely by plotting ln σ vs t according to Eq. (14). A straight line will show that the desorption rate is indeed first order. From the slopes of the straight line taken at various temperatures one may determine the value of E_a and ν independently. A derivation from a linear relationship will in this case be most likely due to the fact that E_a is not constant of the range of σ being measured.

Upon removing the positive bias on the detector during desorption both ions and neutrals will be desorbed. The ratio of the rates of neutral to ion desorption is given by the well known Saha-Langmuir expression

$$\frac{k_a}{k_p} \simeq e^{(I-\phi)/kT}. \qquad (15)$$

At zero Cs coverage, $I-\phi = -1.4$ eV and $T \simeq 800^{\circ}K$ so that $k_a/k_p \simeq 10^{-10}$. Thus, the desorption occurs nearly totally in ionic form. Using Eq. (14) and a value of $\nu = 10^{12}$, a value of $E_p = 1.4$ eV and $E_a = 2.8$ eV, one obtains $\phi = 5.3$ eV which is within experimental error of the value of ϕ generally measured for W(110). Further studies of the ionic desorption spectra at low coverage are being carried out.

SUMMARY

These preliminary results indicate this to be a fruitful method of approach for measuring the adsorption-desorption characteristics from macroscopic single crystal surfaces. Results thus far show a unity sticking coefficient at $T = 77^{\circ}K$ independent of coverage. The desorption spectra of Cs neutrals shows structure indicative of specific states of adsorption rather than a continuous change in binding energy. Terminal coverage desorption of Cs^+ gives $E_p = 1.4$ eV which is generally consistant with the relation $E_p = E_a + I - \phi$. Finally, the $\sigma - \phi$ relationship determined earlier[1] is verified by these studies.

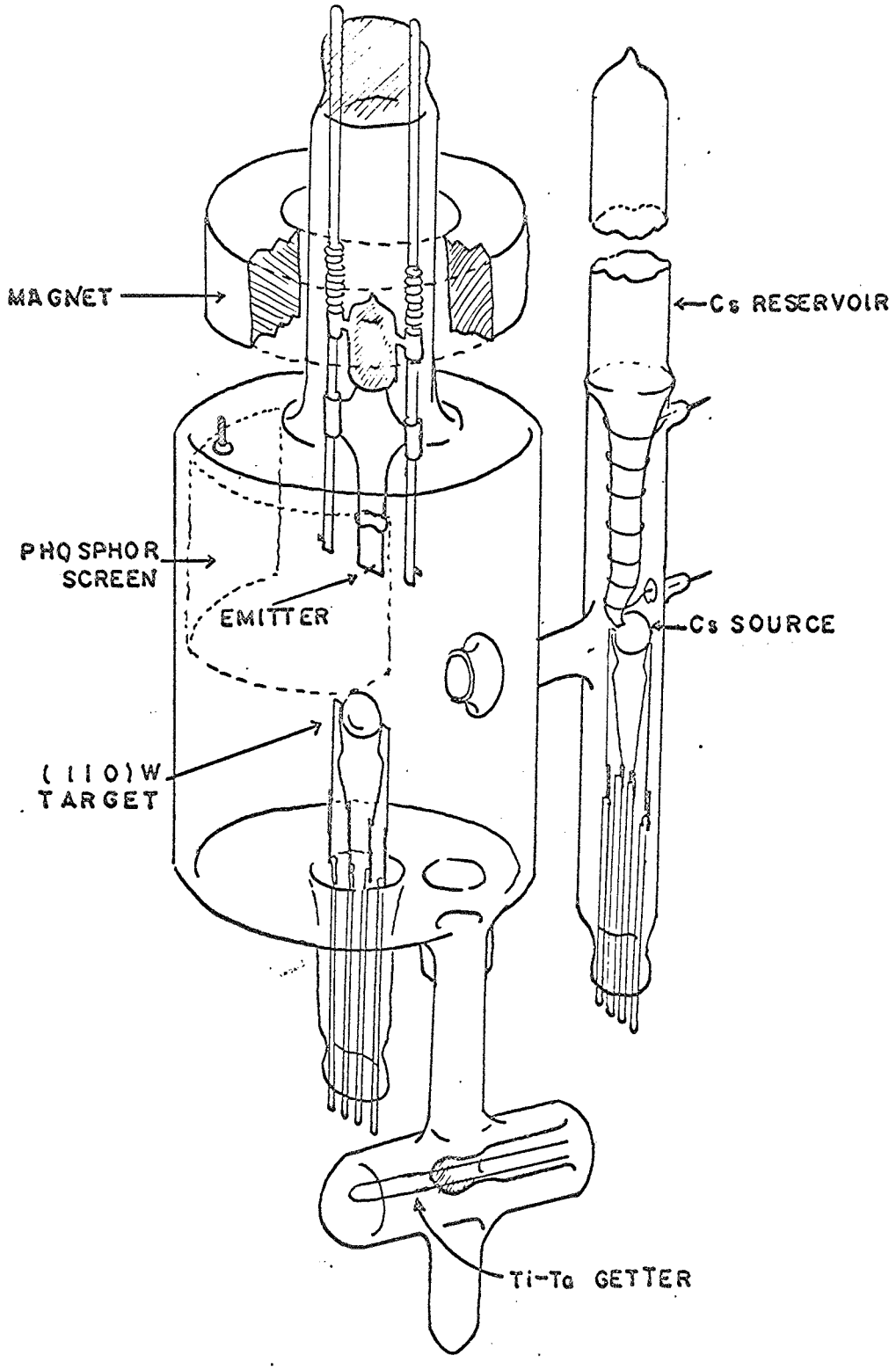

Figure 1. Diagram showing construction of tube for measuring desorption rates and sticking coefficients. By activating the electro-magnet the emitter detector assembly can be moved vertically.

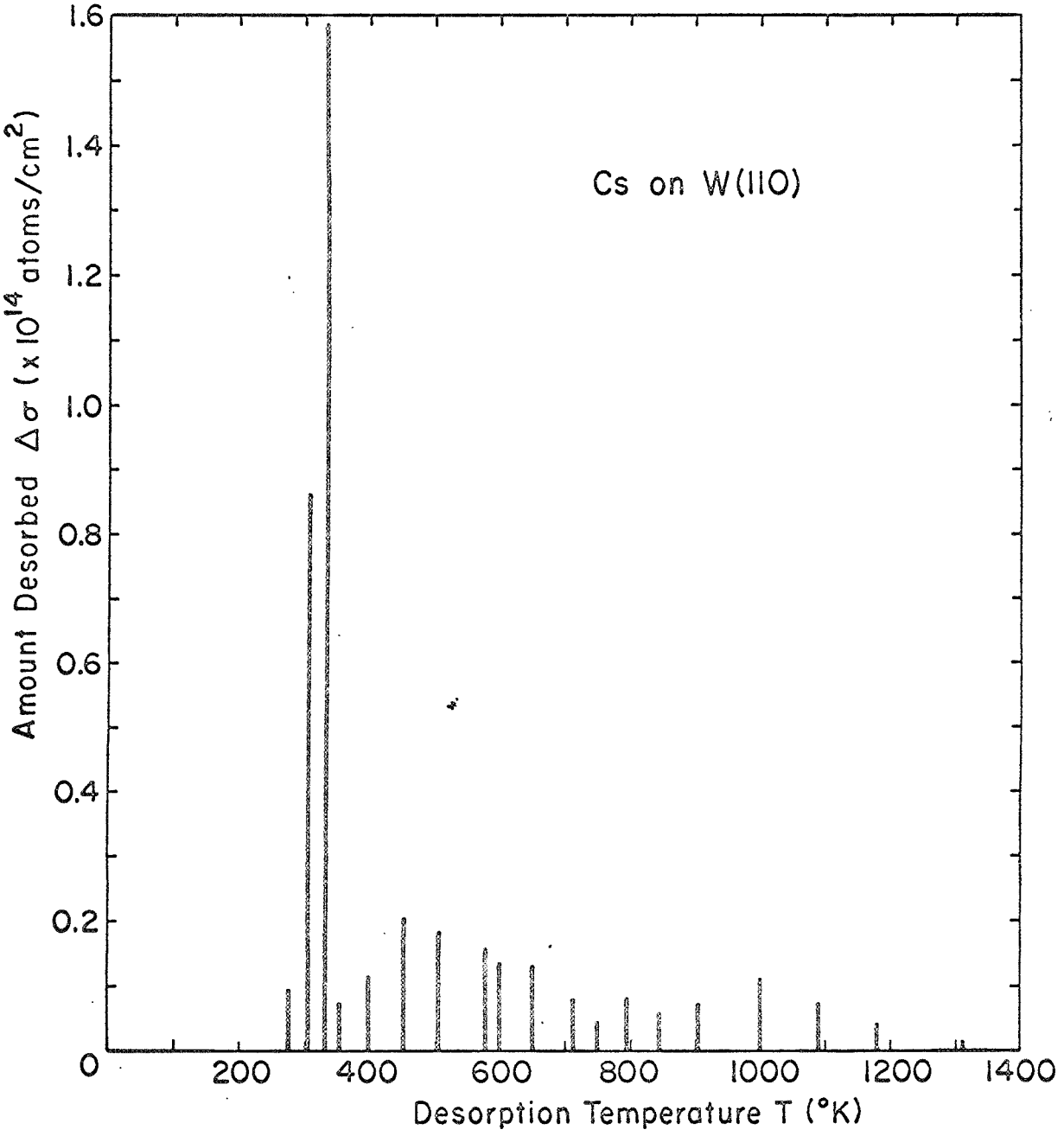

Figure 2. Spectrum shows amount of Cs desorbed from W(110) after heating for 10 sec at the indicated temperature.

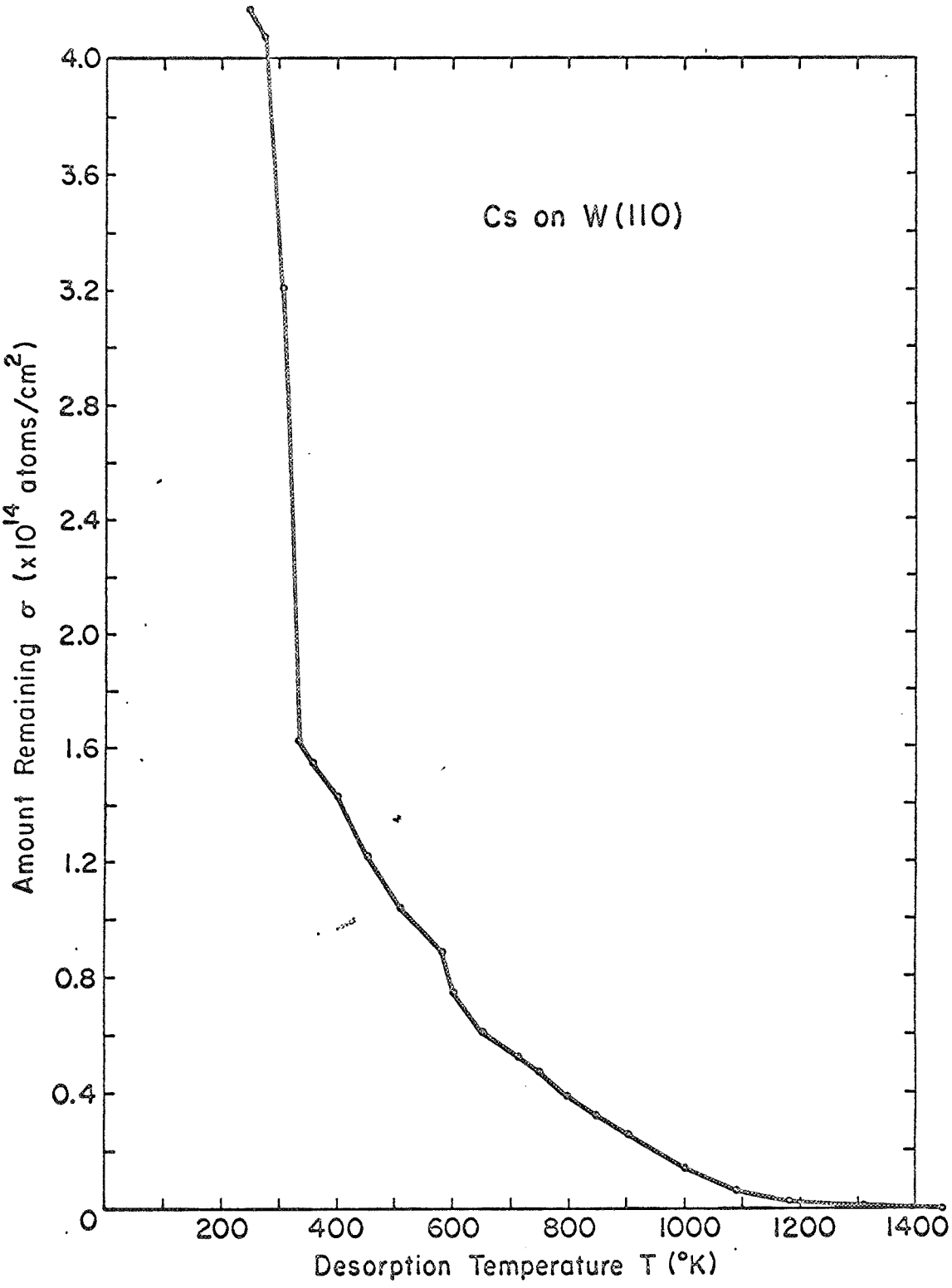

Figure 3. Curve shows the amount of Cs remaining on a W(110) surface after heating for 10 sec at the indicated temperature.

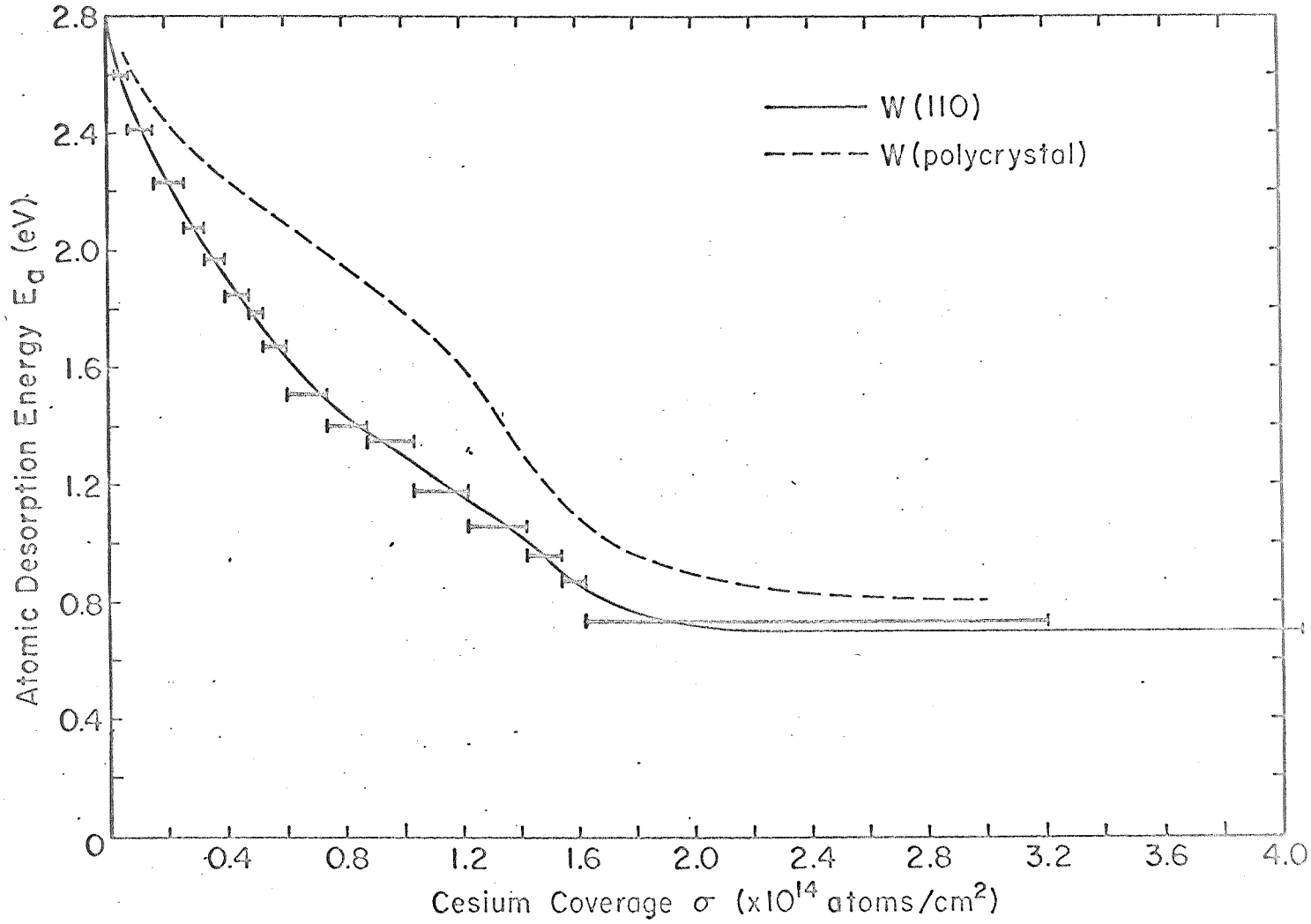

Figure 4. Curve shows the desorption activation energy E_a for neutrals calculated according to Eq. (13) plotted vs Cs coverage. The horizontal bars give the coverage interval.

REFERENCES

1. L.W. Swanson and R.W. Strayer, J. Chem. Phys. 48, 2421 (1968).

2. N.A. Gorbatyi, L.V. Reshetnikova and V.M. Sultanov, Soviet Phys - Solid State 10, 940 (1968).

3. V.M. Gavrilyuk, A.G. Naumovets and A.G. Fedorus, Soviet Physics JEPT 24, 899 (1967).

4. A. Bell and R. Gomer, J. Chem. Phys. 44, 1065 (1966).

5. L.W. Swanson, R.W. Strayer, C.J. Bennette and E.C. Cooper, Final Rep. (NAS CR-54106) for Contr. NAS3-2596, p. 37 (1964).